ASIAN JOURNAL OF FORESTRY
Volume 10, Number 1, June 2026
Pages: 11

E-ISSN: 2580-2844
https://doi.org/10.13057/asianjfor/r100131

Estimating mangrove aboveground biomass using Sentinel-2A Vegetation Indices in a tropical coastal ecosystem on the east coast of North Sumatra, Indonesia

SAMSURI[1,♥], RIZKY AMELIA SIPAHUTAR[1], ANITA ZAITUNAH[2], ARY SAMSURA[3], SUGENG BUDIHARTA[4], BUDI SULISTIOADI[5]

[1]Forest Inventory Laboratory, Faculty of Forestry, Universitas Sumatera Utara. Jl. Lingkar USU, Deli Serdang 20353, North Sumatra, Indonesia. Tel.: +62-61-8211633, ♥email: samsuri@usu.ac.id

[2]Department of Forest Management, Faculty of Forestry, Universitas Sumatera Utara. Jl. Lingkar USU, Deli Serdang 20353, North Sumatra, Indonesia

[3]Center for Urban and Regional Research, Radboud University. Houtlaan 4 6525 XZ Nijmegen, Netherlands

[4]Purwodadi Botanic Gardens, Research Center for Ecology and Ethnobiology, National Research and Innovation Agency. Jl. Surabaya-Malang Km. 65, Pasuruan 67163, East Java, Indonesia

[5]Department of Forest Management, Faculty of Forestry and Tropical Environment, Universitas Mulawarman. Gunung Kelua Campus, Samarinda 75119, East Kalimantan, Indonesia

Manuscript received: 19 October 2025. Revision accepted: 11 April 2026.

Abstract. *Samsuri, Sipahutar RA, Zaitunah A, Samsura A, Budiharta S, Sulistioadi B. 2026. Estimating mangrove aboveground biomass using Sentinel-2A Vegetation Indices in a tropical coastal ecosystem on the east coast of North Sumatra, Indonesia. Asian J For 10 (1): r100131. https://doi.org/10.13057/asianjfor/r100131.* Mangrove forests play a vital role in mitigating climate change by sequestering significant amounts of carbon; however, reliably estimating aboveground biomass (AGB) across large, heterogeneous coastal areas remains challenging. The study evaluates the performance of Sentinel-2A satellite imagery in deriving the Normalized Difference Vegetation Index (NDVI), Green Normalized Difference Vegetation Index (GNDVI), and Transformed Vegetation Index (TVI) for modeling mangrove AGB in the east coast of North Sumatra, Indonesia. A total of 41 field plot samples were integrated with satellite-derived NDVI, GNDVI, and TVI using regression modeling. Regression analyses demonstrate that models based on GNDVI consistently outperform those based on NDVI and TVI. The best-performing model, a GNDVI-based power function ($y = 23.29x^{3.1585}$), achieved an R^2 of 0.60 with a relatively low prediction error (RMSE = 0.70). The spatial application of the selected model revealed an average mangrove AGB of 249.06 t ha^{-1}, with the highest biomass of 510.68 t ha^{-1} in dense stands, indicating a relatively high carbon storage potential. The superior performance of GNDVI is attributed to its greater sensitivity to chlorophyll content in dense, multilayered mangrove canopies, where NDVI tends to saturate. These findings highlight the robustness of GNDVI for estimating mangrove biomass and underscore the utility of Sentinel-2 imagery for carbon stock assessment. The study demonstrates that Sentinel-2-based GNDVI modeling provides a reliable and cost-effective approach for large-scale mangrove biomass estimation, supporting improved carbon assessment and climate mitigation strategies.

Keywords: Blue carbon, carbon absorption, forest inventory, Sentinel-2A, Vegetation Index

INTRODUCTION

Mangrove ecosystems are widely recognized as among the most effective natural carbon sinks globally, sequestering carbon dioxide at rates significantly higher than those of terrestrial forests (Alongi 2012, 2014; Li et al. 2018; Nur et al. 2022). Their considerable biomass, both above- and below-ground, makes them indispensable for climate change mitigation efforts (Hamilton and Friess 2018). However, these critical ecosystems face severe threats from unsustainable exploitation and habitat conversion, undermining their potential for carbon sequestration and other ecological services (Goldberg et al. 2020). In response, carbon trading and blue carbon initiatives have emerged as promising economic incentives to reduce mangrove degradation and promote conservation (Macreadie et al. 2019). However, their success hinges on accurate, large-scale assessments of mangrove carbon stocks, a significant challenge in extensive and often remote coastal regions like Indonesia (Murdiyarso et al. 2015; Simard et al. 2019).

Accurate estimation of aboveground biomass (AGB) is vital for quantifying carbon storage. Remote sensing has become an essential tool for estimating AGB across large and remote coastal areas (Giri 2021; Nuthammachot et al. 2022). Notably, Sentinel-2A imagery offers high spatial resolution, frequent revisit cycles, and red-edge spectral bands sensitive to vegetation structure, thereby increasing its usefulness for mangrove biomass estimation (Li et al. 2021; Nhangumbe et al. 2023). Among various Vegetation Indices (VIs), the Normalized Difference Vegetation Index (NDVI) is the most commonly used proxy for biophysical parameters. Studies applying these VIs in mangroves (e.g., Castillo et al. 2017; Samsuri et al. 2023; Ramadhani et al. 2024) demonstrate their effectiveness, yet a direct comparison of their performance for AGB estimation on Indonesia's east coast, specifically in Sumatra's dense, species-rich mangroves, remains lacking. In dense,

multilayered mangrove canopies with high chlorophyll content, NDVI tends to saturate, decreasing its sensitivity at high biomass levels (Hu et al. 2020). To address this limitation, alternative indices such as the Green Normalized Difference Vegetation Index (GNDVI), which incorporates the green band, and the Transformed Vegetation Index (TVI) have been suggested to improve sensitivity under such conditions (Gitelson and Merzlyak 1998; Suardana et al. 2023).

Despite these advancements, no study has systematically compared the performance of NDVI, GNDVI, and TVI for AGB estimation specifically in the dense, species-rich, naturally regenerated mangroves along the east coast of Sumatra, Indonesia. Furthermore, although hosting one of the largest mangrove areas globally, Indonesia still lacks a site-specific AGB model calibrated for natural mangrove systems on the east coast of Sumatra. Many existing models were developed for plantation mangroves, mixed coastal systems, or regions with different species compositions and stand structures, thereby limiting their transferability to the species-rich, structurally complex Sumatran mangroves. Beyond scientific constraints, in mangrove forest management, there remains a persistent operational gap between developing remote sensing-based biomass models and applying them within forest management units. Previous studies in North Sumatra have either focused on plot-scale direct biomass measurements (e.g., Siregar et al. 2023) or large-scale carbon mapping using satellite imagery (e.g., Thoha et al. 2025), but rarely have they integrated field-based allometric techniques with remote sensing to meet the specific needs of a Protection Forest Management Unit (PFMU). This disconnect reduces the accuracy and usefulness of carbon stock estimates for local forest management and policy implementation.

The mangrove forests managed by the Protection Forest Management Unit (PFMU) along the east coast of Sumatra represent a significant yet under-quantified carbon stock. The spatial distribution and availability of information on its biomass potential are essential for supporting conservation efforts, restoration planning, and participation in global climate change mitigation (Samsuri et al. 2024).

The research gaps are therefore three main areas: (i) lack of a direct comparison among NDVI, GNDVI, and TVI for dense naturally regenerated Sumatran mangroves; (ii) absence of a locally calibrated AGB model for natural, species-rich stands on the east coast of Sumatra; and (iii) disconnection between plot-scale field measurements and landscape-scale remote sensing applications in operational forest management units. Addressing this gap is important because precise, large-scale estimation of mangrove AGB and carbon stock is essential for supporting conservation efforts, restoration planning, and participation in blue carbon trading mechanisms, particularly within the PFMU jurisdiction along the east coast of Sumatra, which represents a large yet under-quantified carbon reservoir. Accordingly, this study contributes directly to addressing these gaps by (i) evaluating the empirical relationship between three Sentinel-2A-derived VIs (NDVI, GNDVI, and TVI) and field-measured AGB; (ii) identifying the most suitable AGB estimation model through regression analysis and validation; (iii) producing spatially explicit maps of AGB and carbon stock for the study area; and (iv) providing a field-based allometric approach that generates stand-level structural information (e.g., diameter distribution) to strengthen the empirical basis for PFMU-level carbon assessment and integration with satellite-based mapping. The specific objectives of this study are to (i) assess the relationship between Vegetation Indices and field-measured mangrove AGB; (ii) identify the most effective biomass estimation model among these indices through regression analysis and validation; and (iii) map the spatial distribution of AGB and carbon stock in the eastern coast of Sumatra's mangrove forests.

MATERIALS AND METHODS

Study area

This research was conducted from March 2021 to May 2021 at PFMU VII, North Sumatra Province, Indonesia. PFMU, as the research location, has a natural mangrove forest. Administratively, the mangrove forest is located in the Panai Hilir Sub-district, Labuhanbatu District, North Sumatra Province. The research location is illustrated in Figure 1. The site research was geographically situated between E 100° 03' 7" - E 100° 32' 17" , and N 3° 32' 17" - N 3 ° 44' 1".

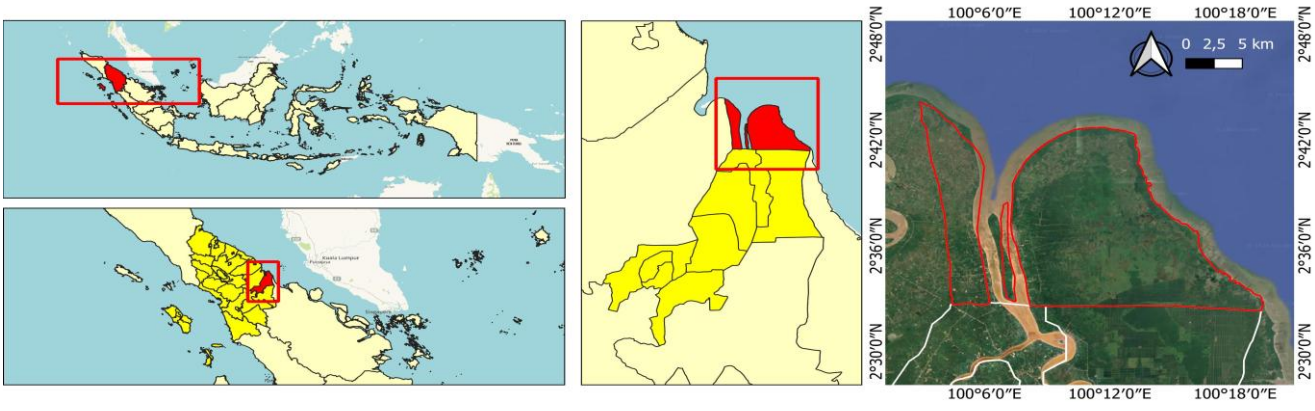

Figure 1. The location of the research site on the eastern coast of North Sumatra, Sumatra Island, Indonesia

Data collecting

Material and tool

The materials used in this study included Sentinel-2A imagery, a mangrove forest map, a working area map, and an administrative map of the Labuhanbatu district. The Sentinel-2 image provides a suitable platform for mangrove management due to its 10-20 m spatial resolution, high temporal resolution (5 days), and availability of red-edge bands sensitive to vegetation structure and chlorophyll dynamics. Other primary data are obtained through field measurements. The tools used include computers, ArcMap 10.3, QGIS 3.16, IBM SPSS 25, Microsoft Excel 2019, a DBH tape to measure diameters, a hypsometer to measure tree height, Global Positioning System (GPS) devices, digital cameras, tally sheets, boats, and stationery.

Field data collecting

Data collection was conducted from 41 field sample plots from April 14 to 24, 2021. Samples were designed based on strata Vegetation Indices; within each strata, samples were placed using the systematic sampling method with a random start. The number of plots placed in each stratum is determined in the stratum's spatial area. This is to ensure that all levels of vegetation density, from sparse to dense mangrove stands, can be represented. The sample plot form was a line strip with a path width of 10 m, carried out in mangrove stands with diameters greater than 10 cm. Non-destructive techniques are used to assess tree biomass. Tree biomass was estimated by measuring the Diameter at Breast Height (DBH, 1.3 m) of mangroves (Sutaryo 2009). The total height of the poles and mangrove trees is measured to calculate biomass. One plot of field sample measuring 10 m x 10 m was placed along the survey path. The field survey path is systematically laid out according to the distribution of Vegetation Index classes, from the lowest to the highest. One plot of this field sample represents 1 pixel of a Vegetation Index map measuring 10 m × 10 m, as indicated by the sample plot's coordinates, which correspond to the central coordinates of that pixel.

Data analysis

Image processing

The Sentinel-2A image level 1C was at the location of Tile 47NME, acquired on 22/02/2021 at 03:27:41.024 GMT, which experiences the lowest tidal conditions. European Space Agency (ESA 2012) states that the Sentinel-2A image classified as Level-1C has been corrected geometrically and radiometrically through the image correction process, which involves a resampling step using QGIS and ArcGIS Atmospheric correction uses the DOS (Dark Object Subtraction) method, which has also been carried out in previous researchers (Huang et al. 2016), aiming to eliminate the darkest pixel value in each band due to atmospheric scattering. Physically based atmospheric corrections are generally more effective than Dark Object Subtraction (DOS) for land cover classification. Sen2Cor demonstrates superior accuracy, while DOS only exceeds uncorrected imagery. Nevertheless, DOS achieves high accuracy in certain scenarios, such as perfect classification for vegetated cropland classes and reasonable performance in scenes with dark objects, including water, vegetation, and urban areas. The DOS method applied to mangrove forests and their surroundings typically involves identifying persistent dark targets, such as deep waters, canopy shadows in mangrove forests, and waterlogged substrates, which allow accurate estimation of radiance paths, especially in wet tropical forests, where weather conditions are relatively homogeneous in a single recording (Bismark et al. 2008; Husna et al. 2018; Latumahina et al. 2021). Under such conditions, DOS has been shown to provide sufficient correction accuracy for Vegetation Index-based analyses, especially when spectral contrast is required in image analysis rather than absolute surface reflectance (Song et al. 2001; Griffin et al. 2024). Since all Vegetation Indices were derived from a single Sentinel-2 acquisition and calibrated using contemporaneous field measurements, these atmospheric effects are assumed to be systematic rather than random. They are largely absorbed within the regression model (Song et al. 2001).

The image was classified to determine the extent of mangrove forest coverage. Land cover classification uses the supervised classification method. Field verification of 225 points to validate the results of the supervised classification. Furthermore, after validation of the classification results, land cover is grouped into two classes: mangrove forest and non-mangrove forest. The kappa accuracy of the land cover classification results for the Sentinel-2A image was 89.07%.

Vegetation Index transformation

This study utilized the NDVI (Normalized Difference Vegetation Index), GNDVI (Green Normalized Difference Vegetation Index), and TVI (Transformed Vegetation Index) methods. These methods are used to determine Vegetation Indices and estimate biomass values. These equations are shown in Table 1.

Table 1. Vegetation Index equation used in the research

Vegetation Index	Equation
NDVI	$\mathrm{NDVI} = \frac{\mathrm{NIR} - \mathrm{RED}}{\mathrm{NIR} + \mathrm{RED}}$
GNDVI	$\mathrm{GNDVI} = \frac{\mathrm{NIR} - \mathrm{GREEN}}{\mathrm{NIR} + \mathrm{GREEN}}$
TVI	$\mathrm{TVI} = \sqrt{\left[\left(\frac{\mathrm{NIR} - \mathrm{RED}}{\mathrm{NIR} + \mathrm{RED}}\right)\right] + 0.5}$

Note: NIR: Band 8, RED: Band 4, GREEN: Band 3

Biomass estimation

Biomass estimation was derived using generalized allometric equations as defined in the Ministry of Forestry's publication, specifically a book on allometric models for estimating tree biomass across diverse forest ecosystems in Indonesia (Krisnawati et al. 2012). The use of a generalized equation was necessary due to the multi-species composition of the mangrove stands and the lack of species-specific allometric models for all taxa present at the study site. The application of a single validated equation provides methodological certainty and consistency across the plot. It can also minimize bias caused by uneven species distribution, a limitation in heterogeneous mangrove ecosystems. A similar approach method has been widely adopted in regional-scale biomass estimation (Hu et al. 2020; Khan et al. 2021). The allometric equation was for each tree individually.

$$W = 0.015\ (D^2H)^{1.08} \quad [1]$$

Where, W is the weight of tree biomass (kg), D is the tree diameter of breast height (cm), and H is the tree height (m)

Regression analysis

Statistical analysis using SPSS software. Statistical tests were performed at the $\alpha = 0.05$ significance level. Therefore, regression coefficients, model F-tests, and pairwise comparisons of model performance were considered statistically significant only when the p-value was less than 0.05.

Regression models were developed to quantify the relationship between field-derived AGB and satellite-based Vegetation Index values (positive Vegetation Index values). The regression analysis employed two variables: Vegetation Index values (NDVI, GNDVI, and TVI) as the independent variable and field-derived AGB data as the dependent variable. Four functional forms-linear, exponential, logarithmic, and power-were evaluated to account for potential nonlinear relationships commonly observed between spectral response and biomass in dense canopies. Model performance was initially assessed using the coefficient of determination (R^2), which indicates the proportion of biomass variance explained by each model.

Linear model

$$y = ax + b \quad [2]$$

Exponential model

$$y = a\ e^{bx} \quad [3]$$

Power model

$$y = ax^b \quad [4]$$

Logarithmic Model

$$y = a\ \ln(x) + b \quad [5]$$

Where:
y: Dependent variable
x: Independent variable
a and b: Coefficients

Each data value is calculated based on its determination coefficient (R^2), and the equation with the highest R^2 is selected. The R^2 value represents the estimation accuracy and proximity of the developed regression model; an R^2 value close to 1 (one) is optimal (Ricke et al. 2019).

Model validation

Cross-validation techniques are commonly used in predictive modeling. However, due to limited sample size (n=41), independent validation was not performed, so this study requires the researcher to prioritize independent statistical metrics (RMSE, Bias, and R^2) for model comparison to avoid excessive dataset partitioning. Model validation uses three complementary metrics: Root Mean Square Error (RMSE), Bias, and R^2. RMSE measures overall prediction error, Bias indicates systematic over- or underestimation, and R^2 reflects explanatory strength. Together, these metrics provide a balanced evaluation of accuracy, precision, and robustness (Hastie et al. 2009; Chai and Draxler 2014). Model selection does not emphasize deriving individual formulas but rather focuses on the comparative interpretability of all metrics. Models with lower RMSE and Bias values and higher R^2 are considered superior. To obtain a proportionally fair comparison, a weighted assessment approach is applied (Saaty 2008). This method assigns equal importance to RMSE, Bias, and R^2. The metric values are normalized to ensure consistency, so that the better-performing model gets a higher score. The optimal model shows the best overall balance between prediction accuracy, minimal systematic error, and high explanatory power, rather than being superior on just one metric.

Root Mean Square Error (RMSE) (Chai and Draxler 2014) is used to identify errors in the model.

$$RMSE = \sqrt{\frac{1}{n}\sum\left(\frac{E-O}{O}\right)^2} \quad [6]$$

Where, E is the biomass value resulting from the regression model, n is the amount of data, o is the value of biomass in the field (t ha^{-1})

Bias (e) (Hastie et al. 2009) is a systematic error resulting from technical errors in the measurement or the measuring instrument used. The agreeable bias value is an e-value close to zero.

$$= \left|\sum\left\{\frac{\left(\frac{E-O}{O}\right)}{n}\right\}\right| x\ 100\% \quad [7]$$

Where, E is the biomass value resulting from the regression model, n is the amount of data, o is the value of biomass in the field (t ha^{-1})

R^2 is a statistical measure that shows how well the independent variables (predictors) in the model explain the variation (change) of the dependent variables (outcomes).

$$R^2 = \frac{\Sigma_{i=1}^{n}(\hat{y}_i - \bar{y}_i)^2}{\Sigma_{i=1}^{n}(y_i - \bar{y})^2} \quad [8]$$

Scoring model. The best model is selected based on RMSE, Bias and R^2 values, which are scored and summed. The model with the highest score is the best and selected model. The scoring formula is generically the Weighted Sum Model (WSM) as below (Belton and Stewart 2002; Saaty 2008):

$$S_i = \frac{\Sigma_{i=1}^{n} w_i x_{ij}}{\Sigma_{j=1}^{n} w_j} \quad [9]$$

Where:
Si: Total score or alternate rating of i (or model i)
Wj: Weight of the j criterion
Xij: The value or score of the i^{th} model on the j^{th} criterion
n: Number of criteria
Index $_i$: Model or alternative to i
index $_j$: Criterion j

The formula determines a model's total score (rating) based on several assessment criteria, with the option to weight each criterion. Each criterion is rated (e.g., on a 1-5 scale) and then multiplied by its weight. The results for all criteria are summed to obtain the final score. The model with the highest Si value is considered the best or most feasible. Test the biomass equation model with three evaluation criteria, namely (i) Root Mean Square Error (RMSE) to measure how big the prediction error is, (ii) Bias to measure the model's tendency to overestimate or underestimate, and (iii) R^2 to measure the closeness of relationships.

Before calculating the total score, the direction of each criterion's preference is determined. The smaller the RMSE and Bias scores, the better; therefore, normalization is applied so that the best score becomes large (positive). The weights for each criterion are equal: 1/3, 1/3, and 1/3. The normalization formula is:

$$X'_{ij} = \frac{X_j^{max} - X_{ij}}{X_j^{max} - X_j^{min}} \text{ and } X'_{ij} = \frac{X_{ij} - X_j^{min}}{X_j^{max} - X_j^{min}} \quad [10]$$

Where X represents the original value of a given metric (RMSE, Bias, or R^2), X_{min} and X_{max} denote the minimum and maximum values of that metric across all evaluated models, and X′ is the normalized value scaled between 0 and 1. For RMSE and Bias, lower values indicate better performance (cost criteria), whereas for R^2, higher values indicate better performance (benefit criterion). Thus, the lowest (best) score will be close to 1, and the highest (worst) will be close to 0.

Mapping biomass and carbon

Biomass distribution maps help visualize how well the selected model represents the field situation. The Power model (G8), $y = 23.29\ x^{3.1585}$, was calculated in QGIS using the Raster Calculator, with GNDVI as the variable x for Sentinel-2 imagery. Carbon stocks are derived from biomass measurements. Carbon stocks are calculated in accordance with the Indonesian National Standard 7724:2011, using a conversion factor of 0.47. The Natural Breaks method divides the biomass and carbon distribution into up to four classes, a technique that naturally separates data classes (Brown 2004).

RESULTS AND DISCUSSION

Mangrove species composition and field-based biomass

Field data collection identified 9 mangrove species at the research site across 41 sample plots. The average aboveground biomass (AGB) differed among species, ranging from 8.10 t ha^{-1} of *Avicennia alba* biomass to 34.44 t ha^{-1} of *Bruguiera parviflora* biomass. Most species exhibited average biomass values between 15 and 30 t/ha (Table 2).

Regression models between Vegetation Indices and biomass

Twelve regression models (G1-G12) were developed using three Vegetation Indices (NDVI, GNDVI, and TVI) and four functional forms (Table 3 and Figure 2). Models based on the GNDVI consistently showed higher coefficients of determination (R^2) than those based on NDVI or TVI, with the highest R^2 (0.60) obtained from exponential (G6) and power (G8) models. NDVI- and TVI-based models showed lower explanatory power, with R^2 values ranging from 0.41 to 0.51 (Table 3).

Model validation and selection of the optimal model

Model validation was performed using RMSE, Bias, and R^2 metrics. Based on this combined ranking of RMSE, Bias, and R^2, the GNDVI power model (G8: $y = 23.29x^{3.1585}$) achieved the highest overall score and was selected for spatial biomass mapping (Table 4).

Table 2. Average of the aboveground biomass each mangrove species in the mangrove forest at the research site

Local name	Scientific name	Average biomass (t Ha^{-1})
Api api	*Avicennia alba* Blume	8.10
Api-api putih	*Avicennia marina* (Forssk.) Vierh.	10.08
Lenggadai	*Bruguiera parviflora* (Roxb.) Wight & Arn. ex Griff.	34.44
Bakau mata buaya	*Bruguiera hainesii* C.G.Rogers	29.19
Bakau minyak	*Rhizophora apiculata* Blume	15.39
Bakau hitam	*Rhizophora mucronata* Lam.	16.87
Singgam	*Scyphiphora hydrophyllacea* C.F.Gaertn.	24.32
Perepat	*Sonneratia alba* Sm.	16.97
Nyirih	*Xylocarpus granatum* J.Koenig	33.04

Table 3. Biomass estimation model and Vegetation Index variable

Vegetation Index	Model equation	Code	Equation	R^2	R^2 adj
NDVI	Linear	G1	$y = 11.685x - 4.8986$	0.41	0.39
	Exponential	G2	$y = 0.0449e^{6.2103x}$	0.50	0.49
	Logarithmic	G3	$y = 6.9965\ln(x) + 5.7198$	0.42	0.40
	Power	G4	$y = 12.677x^{3.7174}$	0.51	0.49
GNDVI	Linear	G5	$y = 13.762x - 4.1312$	0.51	0.50
	Exponential	G6	$y = 0.0724e^{7.1645x}$	0.60	0.59
	Logarithmic	G7	$y = 6.0463\ln(x) + 6.9427$	0.51	0.49
	Power	G8	$y = 23.29x^{3.1585}$	0.60	0.59
TVI	Linear	G9	$y = 24.531x - 23.607$	0.41	0.39
	Exponential	G10	$y = 2E\text{-}06e^{13.037x}$	0.50	0.49
	Logarithmic	G11	$y = 25.73\ln(x) + 0.9042$	0.41	0.39
	Power	G12	$y = 0.9812x^{13.673}$	0.51	0.49

Table 4. The ranking model from the validation test and determination value coefficient

model code	Model	RMSE	Bias	R^2	Normalized RMSE	Bias normalized	R^2 Normalized	Total score	Ranking
G1	Linear	0.76	12.34	0.41	0.3	0.00	0.00	0.10	12
G2	Exponential	0.79	6.09	0.5	0	0.84	0.47	0.44	8
G3	Logarithmic	0.76	12.23	0.42	0.3	0.01	0.05	0.12	9
G4	Power	0.79	5.83	0.51	0	0.87	0.53	0.47	6
G5	Linear	0.69	9.6	0.51	1	0.37	0.53	0.63	3
G6	Exponential	0.71	4.99	0.6	0.8	0.98	1.00	0.93	2
G7	Logarithmic	0.70	9.72	0.51	0.9	0.35	0.53	0.59	4
G8	Power	0.70	4.86	0.6	0.9	1.00	1.00	0.97	1
G9	Linear	0.76	12.3	0.41	0.3	0.01	0.00	0.10	11
G10	Exponential	0.76	6.83	0.5	0.3	0.74	0.47	0.50	5
G11	Logarithmic	0.76	12.27	0.41	0.3	0.01	0.00	0.10	10
G12	Power	0.79	5.84	0.51	0	0.87	0.53	0.47	7

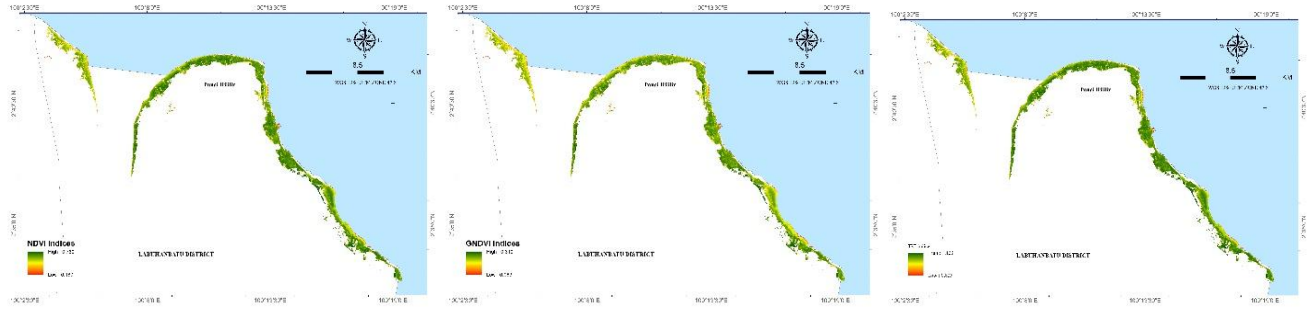

A **B** **C**

Figure 2. Map of Vegetation Index. A. NDVI, B, GNDVI, C. TVI

Spatial distribution of aboveground biomass

The selected GNDVI power model was applied to Sentinel-2A imagery to generate a spatial distribution map of aboveground biomass (Figure 3). The biomass distribution class is divided into 4 classes using the natural breaks method. A method that divides classes naturally in the distribution of data. Estimated AGB values across the study area ranged from 230.51 to 510.68 t ha^{-1}. Most of the mapped area was classified as medium biomass (230.51-308.56 tha^{-1}). Higher biomass values occurred in spatially limited zones, while lower biomass classes occupied a larger proportion of the study area. The mean estimated AGB across the study area was 249.06 t ha^{-1}.

Estimation of carbon stock

The average carbon stock estimate was 114.57 t C ha^{-1}, with a maximum modeled value of 234.91 t C ha^{-1} (Figure 4). Model-based estimates determined an average carbon stock of 114.57 t C ha^{-1}, with a maximum of 234.91 t C ha^{-1} (Figure 4). Spatial patterns of carbon distribution closely followed the modeled biomass distribution.

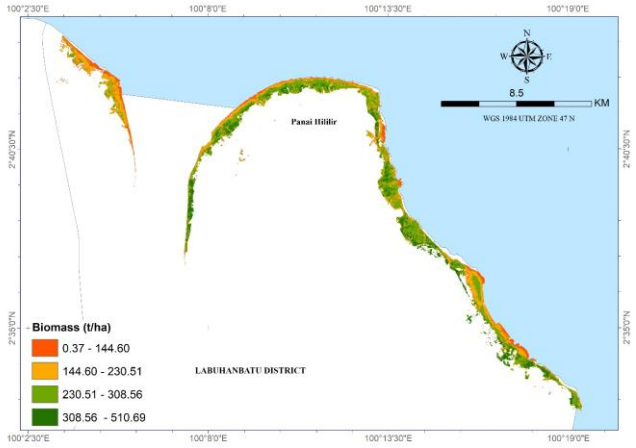

Figure 3. Biomass distribution map based on best model

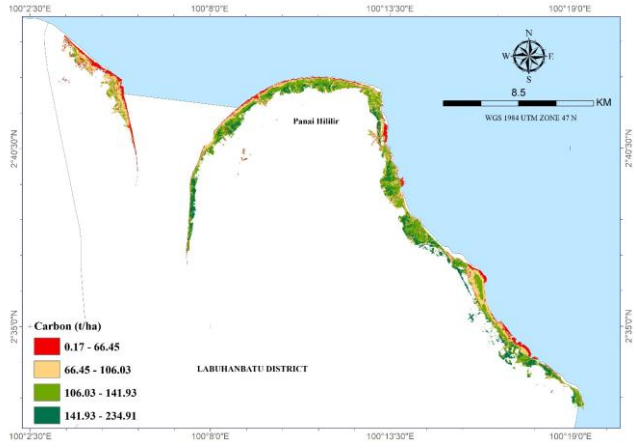

Figure 4. Carbon distribution map derived from biomass model

Discussion

Vegetation Indices in mangrove biomass estimation

The research shows that GNDVI-based models outperformed NDVI- and TVI-based models for estimating AGB in dense mangrove canopies along the east coast of North Sumatra. GNDVI's better performance is probably because it uses the green spectral band, which is more sensitive to changes in chlorophyll content in high-biomass vegetation. In dense, multilayered mangrove canopies like those in this study, the red band in NDVI can saturate, reducing its sensitivity. GNDVI avoids this saturation problem, providing a more reliable indicator of photosynthetic activity and, therefore, biomass (Gitelson and Merzlyak 1998; Gowri and Manjula 2019; Evangelides and Nobajas 2020; Suardana et al. 2023).

The GNDVI-based models consistently outperform NDVI and TVI in estimating aboveground biomass (AGB) in this mangrove ecosystem; it is more than just a technical choice, it has significant scientific and practical implications. Therefore, when using the exponential model (G6), there is a risk of overestimating carbon stocks, especially at higher Vegetation Index values (Foody et al. 2003). However, while using the power model (G8), it can produce more conservative and realistic estimates, especially in dense mangrove ecosystems where saturation effects occur (Mutanga and Skidmore 2004). It was further stated that the power model exhibited lower bias and more stable behavior when applied to spatial mapping, making it more suitable for estimating landscape-level biomass (Chave et al. 2014).

Mangrove forests along North Sumatra's east coast face increasing pressure from land conversion and climate change, yet their ability to store carbon remains poorly quantified at scales relevant to local forest managers. Showing that a simple, publicly available Vegetation Index (GNDVI) applied to Sentinel-2 images can account for 60% of the variation in field-measured biomass provides a cost-effective, easy-to-replicate method for routine biomass monitoring. The moderate but meaningful explanatory power R^2 of 0.60, achieved without complex sensor fusion or extensive field campaigns, is important because it lowers technical barriers for Protected Forest Management Units (PFMU) to establish their own carbon stock baselines, an initial step toward REDD+ readiness and blue carbon finance initiatives. While this level of accuracy does not fully capture all biomass variability, it represents a practical balance between simplicity and reliability, particularly in data-limited contexts.

Chlorophyll-light interactions can explain the superiority of GNDVI over NDVI in dense mangrove canopies. NDVI relies on the red band (around 665 nm), which is strongly absorbed by chlorophyll in the upper canopy. In high-biomass, multilayered stands, the red signal saturates quickly because almost all incident red light is absorbed by the top leaves, making the index insensitive to additional biomass below. In contrast, GNDV utilizes the green band (around 560 nm), where chlorophyll absorption is weaker, and reflectance is more responsive to variations in leaf chlorophyll content across a broader dynamic range. In mangroves, whose canopies are often vertically layered and interspersed with gaps, the green band is more responsive to variation in chlorophyll concentration and canopy structure (Prahesti et al. 2021), responding to differences in foliar chlorophyll that correlate with leaf area index and overall photosynthetic capacity-both direct indicators of biomass. The power model form ($y = 23.29x^{3.1585}$) further enhances the fit because the relationship between spectral reflectance and physical biomass is inherently nonlinear; compared to linear and exponential models (Table 3), the power model showed lower RMSE and bias. A power function captures this diminishing-returns pattern more accurately than a linear or exponential model. The fact that the GNDVI power model also yielded the lowest bias (4.86) and RMSE (0.70) confirms that it not only explains variance but also avoids systematic over- or underestimation across the biomass gradient.

The R^2 of 0.60 achieved here falls within the Sentinel image (10 m × 10 m) reported for similar tropical mangrove studies but occupies an important middle ground. Castillo et al. (2017) reported an R^2 of 0.63 using NDVI in less dense stands, suggesting that NDVI can

perform adequately when canopies are not saturated. However, in denser settings, this study aligns with Lv et al. (2021) and Zhen et al. (2021), who demonstrated GNDVI's extended dynamic range. The power model finding is consistent with Fonton et al. (2017) in the Congo Basin and Búrquez and Martínez-Yrizar (2011) in Sonoran Desert vegetation, both of which recommended nonlinear power functions over log-transformed linear models for unbiased biomass estimation. Notably, the average AGB estimated here (249 t ha^{-1}) is higher than the global average reported by Hu et al. (2020) for Vietnamese mangroves (115 t ha^{-1}) but falls within the 150-400 t ha^{-1} range typical for mature Southeast Asian mangroves (Kauffman and Donato 2012).

The AGB comparison emphasizes that regional allometric calibration remains essential; applying global or non-regional equations would misrepresent carbon stocks in North Sumatra's relatively productive stands. Various Vegetation Indices derived from satellite imagery were used to estimate AGB, including GNDVI using Landsat 8 (Samsuri et al. 2023), and multiple indices combined with SPOT images (Muhd-Ekhzarizal et al. 2018). Some of these AGB models show that GNDVI is more responsive to chlorophyll concentrations across a wider range than the NDVI "red band," making it an accurate tool for biomass assessment (Gitelson and Merzlyak 1998). GNDVI was developed to correlate Leaf Chlorophyll Content (LCC) over a larger dynamic range than NDVI (Zhen et al. 2021). Leaf reflectance strongly influences spectral data, leading satellite readings to appear to show high biomass, especially in plants with high leaf chlorophyll levels.

Aboveground biomass and carbon stock levels

The estimated average biomass of 249.06 t ha^{-1} obtained in this study is comparable to reported values in Southeast Asian mangrove ecosystems, which typically range from 150 to 400 t ha^{-1} depending on species composition and age of establishment (Kauffman and Donato 2012; Hu et al. 2020). The variability of aboveground biomass observed across the study area represents differences in mangrove forest structure and species composition. Field measurements show that species with larger strata and larger trunk dimensions account for a disproportionate share of total biomass. This condition generally shows a pattern common in natural mangrove systems (Krisnawati et al. 2012; Rastogi et al. 2021). For example, the observed variations are consistent with the development of mangrove zones and stands along tropical coastlines (Onrizal and Kusmana 2008; Alongi 2012, 2014).

Ecologically, the spatial heterogeneity shown in the GNDVI-derived biomass map mosaics, with medium- and high-biomass patches mixed with low-biomass zones, reflects underlying gradients in tidal flooding, salinity, and species competition. Similar spatial heterogeneity has been documented in mangrove forests across Southeast Asia and reflects the combined influence of stand density (Muhd-Ekhzarizal et al. 2018; Nguyen et al. 2019; Hu et al. 2020). This spatial pattern is important because it identifies natural refuges with high carbon density that should be targeted for conservation. From a management perspective, the study offers PFMU VII a practical tool: the validated GNDVI power model can be applied to any new Sentinel-2 image with less recalibration, enabling annual tracking of biomass changes. For example, a decrease in predicted biomass in a previously high-biomass area would indicate degradation (such as from illegal harvesting or hydrologic changes), prompting early action. Conversely, low-biomass zones can be targeted for restoration using species suited to local conditions. Assuming a standard carbon fraction of 0.47 (Badan Standardisasi Nasional (BSN 2011)), which may vary depending on species composition (using SNI 7724:2011 factor of 0.47), results in an average of 115 t C ha^{-1}, which is directly used for national greenhouse gas inventory reporting. By integrating this method into routine forest monitoring, Indonesia's forest management units can shift from occasional, project-based carbon assessments to operational, satellite-based systems-an essential step for expanding blue carbon conservation.

Implications for management and conservation

The biomass spatial information generated in this study can support forest management units in identifying priority conservation zones, evaluating restoration success, monitoring biodiversity, and taking initial steps toward REDD+ readiness through carbon calculations under national climate mitigation programs such as REDD+ and blue carbon initiatives. The spatially explicit biomass and carbon stock maps produced by the study provide practical decision-support tools for mangrove forest management and conservation (Winkel et al. 2022). Mangrove forest areas identified as having high-biomass zones represent significant carbon reservoirs and biodiversity assets and should be prioritized for conservation and protection (Goldberg et al. 2020). Conversely, mangrove forest areas with consistently low biomass or carbon can be targeted for restoration and rehabilitation, enabling more efficient allocation of available management resources (Nuthammachot et al. 2022).

The use of Sentinel-2 imagery combined with a single Vegetation Index-based model offers a cost-effective framework for routine monitoring (Awaliyan and Sulistioadi 2018; Drupadi et al. 2021; Matangaran et al. 2024). Repeated application of the validated GNDVI model allows the Forest Management Unit to detect temporal changes in biomass, supporting early identification of degradation or recovery processes (Giri 2021; Samsuri et al. 2024). This approach corresponds with national forest monitoring systems and supports reporting requirements for climate mitigation initiatives such as REDD+ and blue carbon programs (Calvin et al. 2023).

Limitations and future research

Several limitations have been identified when using the allometric equation for biomass estimation. The use of a generalized allometric equation, while necessary for mixed-mangrove species, may introduce uncertainty in species-specific biomass estimates (Komiyama et al. 2008; Alvarez et al. 2012; Krisnawati et al. 2012). The study used general allometric equations to accommodate the composition of mangrove stands, which may introduce

uncertainty because mangrove species differ substantially in growth form, wood density, and canopy architecture. Species belonging to the genera *Rhizophora*, *Bruguiera*, and *Sonneratia*, for example, often exhibit contrasting stem-shape and biomass-allocation patterns, which can lead to systematic deviations when a single general equation is applied (Komiyama et al. 2005; Kauffman and Donato 2012).

Wood density is a key factor contributing to variability in biomass estimation. Mangrove species exhibit significant interspecific differences in wood density, which directly influence the relationship between tree diameter and biomass accumulation. Biomass estimates that ignore species-specific wood densities can lead to overestimations, particularly in structurally diverse tropical forests (Chave et al. 2014). For instance, species like *Xylocarpus granatum* and *Bruguiera* spp. generally have denser wood than *Avicennia* species, meaning trees of the same diameter can store different amounts of biomass.

Variability in tree height also contributes to uncertainty in biomass estimates. Height variation affects biomass allocation and canopy architecture, so including tree height as an additional predictor can significantly improve the accuracy of biomass estimates and reduce model errors in tropical forests (Forrester 2021). However, measuring the height of trees in dense mangrove stands is operationally challenging. These factors together highlight the inherent trade-offs between operational feasibility and model precision in large-scale biomass estimation. Although general allometric equations remain widely used in the assessment of relatively large areas, future studies should prioritize the development of species-specific models or regional calibrations that combine wood density and structural variables such as tree height. Such an improvement in allometric equations can reduce uncertainty and improve the accuracy of biomass and carbon stock estimates in structurally complex mangrove ecosystems. Integrating field-based allometric measurements with remote sensing approaches is increasingly recommended to reduce uncertainty in mangrove biomass estimation and to improve regional carbon stock assessments.

The difference in the time of image acquisition and field measurement allows for differences in biomass estimation results. However, the mangrove forest studied is an evergreen forest, so the biomass will not change significantly in 2 months. This mangrove forest is a protected natural area, so its ecological condition is relatively stable. Additionally, the VI is more sensitive to canopy cover than to short-term changes in biomass. The 10 m resolution of Sentinel-2 may not fully capture the fine-scale heterogeneity of mangrove forests, potentially leading to underestimation in very high-density patches (Hu et al. 2020). To improve the allometric model, future research should prioritize the development of region- and species-specific allometric models and explore integrating complementary remote sensing data, such as LiDAR or Synthetic Aperture Radar (SAR), to enhance structural characterization (Fonton et al. 2017; Nuthammachot et al. 2022). Multi-sensor data fusion and advanced modeling approaches are expected to further enhance the accuracy of biomass estimation in complex mangrove ecosystems.

In conclusion, the study successfully evaluated the Vegetation Index derived from Sentinel-2A to estimate the aboveground biomass (AGB) of mangrove forests along the east coast of North Sumatra, Indonesia, using field measurements from 41 plots. Among the indices and regression forms tested, the GNDVI-based power model ($y = 23.29x^{3.1585}$) had the best overall performance. The model achieves a moderate determination coefficient ($R^2 = 0.60$), a relatively low prediction error (RMSE $\approx$ 0.70), and minimal bias, demonstrating balanced performance across validation metrics. These results show that GNDVI provides a more responsive spectral indicator for biomass estimation in dense mangrove canopies compared to NDVI and TVI. The spatial application of the selected model showed that the mangrove forests in the study area contained potential biomass stocks, with estimated AGB ranging from around 230 to 511 t ha^{-1} and an average of 249.06 t ha^{-1}. The average carbon stock is estimated at 114.57 t C ha^{-1}, with higher values concentrated in relatively limited high-density stands. These findings offer valuable insights into progress in remote sensing-based biomass estimation. They demonstrate the robustness of a GNDVI-driven power model for tropical mangrove ecosystems using medium-resolution satellite data, and can support mangrove monitoring, carbon stock evaluation, and climate mitigation in coastal areas with limited data. Overall, this study indicates that Sentinel-2-based Vegetation Index models serve as useful tools for regional mangrove biomass assessment. However, the results should be viewed with caution due to model uncertainty, the use of generalized allometric equations, and the limited spatial resolution of Sentinel-2A data.

REFERENCES

Alongi DM 2014. Carbon cycling and storage in mangrove forests. Ann Rev Mar Sci 6: 195-219. https://doi.org/10.1146/annurev-marine-010213-135020.

Alongi DM. 2012. Carbon sequestration in mangrove forests. Carbon Manag 3 (3): 313-322. https://doi.org/10.4155/cmt.12.20.

Alvarez E, Duque A, Saldarriaga J, Cabrera K, de las Salas G, del Valle I, Lema A, Moreno F, Orrego S, Rodríguez L. 2012. Tree aboveground biomass allometries for carbon stocks estimation in the natural forests of Colombia. For Ecol Manag 267: 297-308. https://doi.org/10.1016/j.foreco.2011.12.013.

Awaliyan MR, Sulistioadi YB. 2018. Land cover classification on Sentinel-2A satellite imagery using tree algorithm method. ULIN Jurnal Hutan Tropis 2 (2): 98-104. https://doi.org/10.32522/u-jht.v2i2.1363.

Badan Standardisasi Nasional (BSN). 2011. SNI 7724:2011 tentang Pengukuran dan Penghitungan Cadangan Karbon-Pengukuran Lapangan untuk Penaksiran Cadangan Karbon Hutan. BSN, Jakarta. [Indonesian]

Belton V, Stewart TJ. 2002. Multiple Criteria Decision Analysis: An Integrated Approach. Springer, Boston. https://doi.org/10.1007/978-1-4615-1495-4.

Bismark MN, Heriyanto, Iskandar S. 2008. Biomass and carbon content in production forests in Siberut Island Biosphere Reserve, West Sumatra. Jurnal Penelitian Hutan dan Konservasi Alam 5 (5): 397-407. https://doi.org/10.20886/jphka.2008.5.5.397-407.

Brown G. 2004. Mapping spatial attributes in survey research for natural resource management: Methods and applications. Soc Nat Resour 18 (1): 17-39. https://doi.org/10.1080/08941920590881853.

Búrquez A, Martínez-Yrízar A. 2011. Accuracy and bias on the estimation of aboveground biomass in the woody vegetation of the Sonoran Desert. Botany 89 (9): 625-633. https://doi.org/10.1139/B11-050.

Calvin K, Dasgupta D, Krinner G, Mukherji A, Thorne PW, Trisos C, Hoesung L, Jose R, Paulina A, Ko B, Gabriel B, William C, Sarah C, Fatima D, Aïda D-N, David D, Matthias G, Oliver G, Bronwyn H, Zinta Z. 2023. Climate Change 2023: Synthesis Report. Contribution of Working Groups I, II and III to the Sixth Assessment Report of the Intergovernmental Panel on Climate Change. Lee H, Romero J (eds.). IPCC, Geneva, Switzerland.

Castillo JAA, Apan AA, Maraseni TN, Salmo SG. 2017. Estimation and mapping of aboveground biomass of mangrove forests and their replacement land uses in the Philippines using Sentinel imagery. ISPRS J Photogramm Remote Sens 134: 75-85. https://doi.org/10.1016/j.isprsjprs.2017.10.016.

Chai T, Draxler RR. 2014. Root Mean Square Error (RMSE) or Mean Absolute Error (MAE)? Arguments against avoiding RMSE in the literature. Geosci Model Dev 7 (3): 1247-1250. https://doi.org/10.5194/gmd-7-1247-2014.

Chave J, Réjou-Méchain M, Búrquez A et al. 2014. Improved allometric models to estimate the aboveground biomass of tropical trees. Glob Chang Biol 20 (10): 3177-3190. https://doi.org/10.1111/gcb.12629.

Drupadi TA, Ariyanto DP, Suladi. 2021. Estimating biomass and carbon levels stored on various slopes and land cover at Mount Bromo UNS KHDTK. J Agric 32 (2): 112-119. https://doi.org/10.24198/agrikultura.v32i2.32344.

European Space Agency (ESA). 2012. Sentinel-2: ESA's Optical High-Resolution Mission for GMES Operational Services. ESA SP-1322/2. ESA, Noordwijk, The Netherlands.

Evangelides C, Nobajas A. 2020. Red-edge Normalised Difference Vegetation Index ($NDVI_{705}$) from Sentinel-2 imagery to assess post-fire regeneration. Remote Sens Appl Soc Environ 17: 100283. https://doi.org/10.1016/j.rsase.2019.100283.

Fonton NH, Medjibe VP, Djomo AN, Kondaoulé J, Rossi V, Ngomanda A, Maidou HM. 2017. Analyzing accuracy of the power functions for modeling aboveground biomass prediction in Congo Basin tropical forests. Open J For 7 (4): 388-402. https://doi.org/10.4236/ojf.2017.74023.

Foody GM, Boyd DS, Cutler MEJ. 2003. Predictive relations of tropical forest biomass from Landsat TM data and their transferability between regions, Remote Sens. Environ. 85 (4): 463-474. https://doi.org/10.1016/S0034-4257(03)00039-7.

Forrester DI. 2021. Does individual-tree biomass growth increase continuously with tree size? For Ecol Manag 481: 118717. https://doi.org/10.1016/j.foreco.2020.118717.

Giri C. 2021. Recent advancement in mangrove forests mapping and monitoring of the world using Earth observation satellite data. Remote Sens 13 (4): 563. https://doi.org/10.3390/rs13040563.

Gitelson A, Merzlyak M. 1998. Remote sensing of chlorophyll concentration in higher plant leaves. Adv Space Res 22 (5): 689-692. https://doi.org/10.1016/S0273-1177(97)01133-2.

Goldberg L, Lagomasino D, Thomas N, Fatoyinbo T. 2020. Global declines in human-driven mangrove loss. Glob Chang Biol 26 (10): 5844-5855. https://doi.org/10.1111/gcb.15275.

Gowri L, Manjula KR. 2019. Evaluation of various Vegetation Indices for multispectral satellite images. Intl J Innov Technol Explor Eng 8 (10): 3494-3500. https://doi.org/10.35940/ijitee.J9195.0881019.

Griffin R, Robinson G, Williams A. 2024. Advances in satellite monitoring of coastal ecosystems: A decade of Sentinel-2. Remote Sens Environ 302: 113965. https://doi.org/10.1016/j.rse.2023.113965.

Hamilton SE, Friess DA. 2018. Global carbon stocks and potential emissions due to mangrove deforestation from 2000 to 2012. Natur Clim Chang 8: 240-244. https://doi.org/10.1038/s41558-018-0090-4.

Hastie T, Tibshirani R, Friedman J. 2009. The Elements of Statistical Learning: Data Mining, Inference, and Prediction. 2nd edition. Springer Series in Statistics, New York. https://doi.org/10.1007/978-0-387-84858-7.

Hu T, Zhang Y, Su Y, Zheng Y, Lin G, Guo Q. 2020. Mapping the global mangrove forest aboveground biomass using multisource remote sensing data. Remote Sens 12 (10): 1690. https://doi.org/10.3390/rs12101690.

Huang H, Roy DP, Boschetti L, Zhang HK, Yan L, Kumar SS, Gomez-Dans J, Li J. 2016. Separability Analysis of Sentinel-2A Multi-Spectral Instrument (MSI) Data for Burned Area Discrimination. Remote Sens 8 (10): 873. https://doi.org/10.3390/rs8100873.

Husna VN, Siregar VP, Agus SB, Arifin T. 2018. Estimation of above-surface biomass carbon stocks in mangrove stands using remote sensing in Tongke-Tongke, South Sulawesi. J Nat Resour Environ Manag 9 (2): 456-466. https://doi.org/10.29244/jpsl.9.2.456-466.

Kauffman JB, Donato DC. 2012. Protocols for the Measurement, Monitoring and Reporting of Structure, Biomass and Carbon Stocks in Mangrove Forests. Center for International Forestry Research, Bogor. https://doi.org/10.17528/cifor/003749.

Khan IA, Khan WR, Ali A, Nazre M. 2021. Assessment of aboveground biomass in Pakistan forest ecosystem's carbon pool: A review. Forests 12 (5): 586. https://doi.org/10.3390/f12050586.

Komiyama A, Ong JE, Poungparn S. 2008. Allometry, biomass, and productivity of mangrove forests: A review. Aquat Bot 89 (2): 128-137 https://doi.org/10.1016/j.aquabot.2007.12.006.

Komiyama A, Poungparn S, Kato S. 2005. Common allometric equations for estimating the tree weight of mangroves. J Trop Ecol 21 (4):471-477. https://doi.org/10.1017/S0266467405002476.

Krisnawati H, Rev CA, Rinaldi I. 2012. Monograph of Allometric Models for Estimating Tree Biomass in Various Types of Forest Ecosystems in Indonesia. Center for Forestry Research and Development, Bogor.

Latumahina F, Mardiatmoko G, Passal AI, Kartikawati NK. 2021. The potency of biomass and carbon stocks under agroforestry dusung areas in Maluku, Indonesia. Intl J Adv Sci Eng Inf Technol 11 (5): 1935-1942. https://doi.org/10.18517/ijaseit.11.5.12324.

Li C, Zhou L, Xu W. 2021. Estimating aboveground biomass using Sentinel-2 MSI data and ensemble algorithms for grassland in the Shengjin Lake Wetland, China. Remote Sens 13 (8): 1595. https://doi.org/10.3390/rs13081595.

Li SB, Chen PH, Huang JS, Hsueh ML, Hsieh LL, Lee CL, Lin HJ. 2018. Factors regulating carbon sinks in mangrove ecosystems. Glob Chang Biol 24 (9): 4195-4210. https://doi.org/10.1111/gcb.14322.

Lv T, Zhou X, Tao Z, Sun X, Wang J, Li R, Xie F. 2021. Remote sensing-guided spatial sampling strategy over heterogeneous surface ground for validation of Vegetation Indices products with medium and high spatial resolution. Remote Sens 13 (14): 2674. https://doi.org/10.3390/rs13142674.

Macreadie PI, Anton A, Raven JA et al. 2019. The future of Blue Carbon science. Nat Commun 10 :3998. https://doi.org/10.1038/s41467-019-11693-w.

Matangaran JR, Barokah SM, Mujahid M, Trison S, Putra EI. 2024. Change of carbon mass after timber harvesting in a natural forest, West Sumatra Indonesia. IOP Conf Ser Earth Environ Sci 1315: 012040. https://doi.org/10.1088/1755-1315/1315/1/012040.

Muhd-Ekhzarizal ME, Mohd-Hasmadi I, Hamdan O, Mohamad-Roslan MK, Noor-Shaila S. 2018. Estimation of aboveground biomass in mangrove forests using Vegetation Indices from SPOT-5 image. J Trop For Sci 30 (2): 224-233. https://doi.org/10.26525/JTFS2018.30.2.224233.

Murdiyarso D, Purbopuspito J, Kauffman JB, Warren MW, Sasmito SD, Donato DC, Manuri S, Krisnawati H, Taberima S, Kurnianto S. 2015. The potential of Indonesian mangrove forests for global climate change mitigation. Natur Clim Chang 5: 1089-1092. https://doi.org/10.1038/nclimate2734.

Mutanga O, Skidmore AK. 2004. Narrow band Vegetation Indices overcome the saturation problem in biomass estimation. Intl J Remote Sens 25 (19): 3999-4014. https://doi.org/10.1080/01431160310001654923.

Nguyen LD, Nguyen CT, Le HS, Tran BQ. 2019. Mangrove mapping and aboveground biomass change detection using satellite images in coastal areas of Thai Binh Province, Vietnam. For Soc 3 (2): 248-261. https://doi.org/10.24259/fs.v3i2.7326.

Nhangumbe M, Nascetti A, Ban Y. 2023. Multi-temporal Sentinel-1 SAR and Sentinel-2 MSI data for flood mapping and damage assessment in Mozambique. ISPRS Intl J Geo-Inf 12 (2): 53. https://doi.org/10.3390/ijgi12020053.

Nur AAI, Arifiani KN, Ramadhandi AR, Sabrina AD, Nugroho GD, Kusumaningrum L, Ramdhun D, Bao TQ, Yap CK, Budiharta S, Setyawan AD. 2022. Estimation of aboveground biomass and carbon stock in Damas Beach, Trenggalek District, East Java, Indonesia. Indo Pac J Ocean Life 6: 80-86. https://doi.org/10.13057/oceanlife/o060203.

Nuthammachot N, Askar A, Stratoulias D, Wicaksono P. 2022. Combined use of Sentinel-1 and Sentinel-2 data for improving above-ground biomass estimation. Geocarto Intl 37 (2): 366-376. https://doi.org/10.1080/10106049.2020.1726507.

Onrizal, Kusmana C. 2008. Ekologi hutan mangrove di Pantai Timur Sumatera Utara. Biodiversitas 9 (1): 25-29. https://doi.org/10.13057/biodiv/d090107. [Indonesian]

Prahesti K, Malaka R, Sudirman B. 2021. Stamina prediction of cows and goats stamina prediction of cows and goats to exercise changes by measuring body temperature, heart rate, and respiratory rate. Hasanuddin J Anim Sci 3 (1): 1-7. https;//doi.org/10.20956/hajas.v3i1.14130.

Ramadhani G, Wahyuningtyas J, Arifiandita DM, Ayuningtyas HR, Deristani A, Ulumuddin YI, Setyawan AD. 2024. Mangrove dynamics on the Madura Island coast, Indonesia, analyzed through NDVI: Balancing degradation and restoration efforts. Indo Pac J Ocean Life 8: 101-111. https://doi.org/10.13057/oceanlife/o080205.

Rastogi RP, Phulwaria M, Gupta DK. 2021. Mangroves: Ecology, Biodiversity and Management. Springer Nature, New Delhi. https://doi.org/10.1007/978-981-16-2494-0.

Ricke K, Drouet L, Caldeira K, Tavoni M. 2019. Author correction: Country-level social cost of carbon. Nat Clim Chang 9 (7): 567. https://doi.org/10.1038/s41558-019-0455-3.

Saaty TL. 2008. Decision Making with the Analytic Hierarchy Process. Springer, New York. https://doi.org/10.13128/Aestimum-7138.

Samsuri S, Abdillah MR, Zaitunah A, Utomo B, Sulistioadi YB. 2024. Distribution of density and zoning patterns of mangrove forest in Eastern Coastal Sumatera, Indonesia. IOP Conf Ser Earth Environ Sci 1352 (1): 012045. https://doi.org/10.1088/1755-1315/1352/1/012045.

Samsuri S, Pasaribu SN, Zaitunah A, Ahmad AG, Yunasfi, Dalimunthe A, Sulistioadi JB. 2023. The Aboveground Biomass Model of Mangrove Forest in Panai Hilir, Indonesia. IOP Conf Ser Earth Environ Sci 1277 (1): 012001. https://doi.org/10.1088/1755-1315/1277/1/012001.

Simard M, Fatoyinbo TE, Smetanka C, Rivera-Monroy VH, Castañeda-Moya E, Thomas N, Van der Stocken T. 2019. Mangrove canopy height globally related to precipitation, temperature and cyclone frequency. Natur Geosci 12: 40-45. https://doi.org/10.1038/s41561-018-0279-1.

Siregar AS, Nasution Z, Rahmawaty. 2023. Estimation of carbon stocks on mangrove forests at Pulau Kampai using destructive and non-destructive methods. Tunas Geografi 12 (1): 33-46. https://doi.org/10.24114/tgeo.v12i1.47945.

Song C, Woodcock CE, Seto KC, Lenney MP, Macomber SA. 2001. Classification and change detection using Landsat TM data: When and how to correct atmospheric effects? Remote Sens Environ 75 (2): 230-244. https://doi.org/10.1016/S0034-4257%2800%2900169-3.

Suardana AA, Anggraini N, Nandika MR, Aziz K, As-Syakur AR, Ulfa A, Wijaya AD, Prasetio W, Winarso G, Dewanti R. 2023. Estimation and mapping aboveground mangrove carbon stock using Sentinel-2 data derived Vegetation Indices in Benoa Bay of Bali Province, Indonesia. For Soc 7 (1): 116-134. https://doi.org/10.24259/fs.v7i1.22062.

Sutaryo D. 2009. Penghitungan Biomasa. Wetlands International Programmer, Bogor. [Indonesian]

Thoha AS, Purwanto, Wijayanti P, Noviani R, Prasad RR, Nasibah SP. 2025. Mapping aboveground carbon of mangroves using Sentinel-2 satellite imagery in the east coast of North Sumatra Province, Indonesia. Biodiversitas 26 (8): 3916-3925. https://doi.org/10.13057/biodiv/d260822.

Winkel G, Lovrić M, Muys B, Pia K, Thomas L, Mireia P, Davide P, Nathalie P, Tobias P, Irina P, Constanza P, Helga P, Dennis R, Jeanne-Lazya R, Bo T, Liisa T, Mario T, Harald V, Gerhard W, Sven W. 2022. Governing Europe's forests for multiple ecosystem services: Opportunities, challenges, and policy options. For Policy Econ 145: 102849. https://doi.org/10.1016/j.forpol.2022.102849.

Zhen J, Jiang X, Xu Y, Miao J, Zhao D, Wang J, Wang J, Wu G. 2021. Mapping leaf chlorophyll content of mangrove forests with Sentinel-2 images of four periods. Intl J Appl Earth Obs Geoinf 102: 102387. https://doi.org/10.1016/j.jag.2021.102387.